Evaluation of biofouling characteristics on reverse osmosis membranes of disinfection-residual-bacteria (DRB) after seven kinds of disinfection

Yin-Hu Wu (wuyinhu@mail.tsinghua.edu.cn)
Tsinghua University
Haobin Wang
https://orcid.org/0000-0002-2003-131X
Wen-Long Wang
Tsinghua University
Li-Wei Luo
Tsinghua University
Gen-Qiang Chen
Tsinghua University
Zhuo Chen
Tsinghua University
Song Xue
Tsinghua University
Ao Xu
Research Institute for Environmental Innovation (Suzhou)
Yu-Qing Xu
Tsinghua University
Nozomu Ikuno
Kurita Water Industries Ltd.
Kazuki Ishii
Kurita Water Industries Ltd.
Hongying Hu
Tsinghua University

Article

Keywords: Disinfection-residual-bacteria (DRB), Biofilm, Membrane fouling, Microbial community, Disinfection

Posted Date: July 13th, 2022

DOI: https://doi.org/10.21203/rs.3.rs-1811963/v1

Version of Record: A version of this preprint was published at npj Clean Water on March 21st, 2023. See the published version at https://doi.org/10.1038/s41545-023-00240-2.

Abstract

Biofouling is a critical defect of the reverse osmosis (RO) system. It has been reported that disinfection processes tend to select certain undesirable disinfection-residual bacteria (DRB), leading to severe long-term biofouling potential. To provide constructive guidance on biofouling prevention in RO systems, this study evaluated the biofouling characteristics of RO membranes of DRB after the application of five mature disinfection methods (NaClO, NH_2Cl, ClO_2, UV, and O_3) and two novel disinfection methods (K_2FeO_4 and flow-through electrode system (FES)). After a 32-day biofilm cultivation on the RO membranes, the DRB biofilm of K_2FeO_4 and O_3 caused a slight normalised flux drop (22.4 ± 2.4% and 23.9 ± 1.7%, respectively) of RO membrane compared with the control group (non-disinfected, ~ 27% normalised flux drop). Moreover, the biofouling degree of the NH_2Cl-DRB biofilm was similar to that of the control group. The remaining disinfection types aggravated membrane biofouling. The biofouling behaviour of DRB showed no relationship with bacterial concentration or activity. The thickness and density of the biofilms as well as the organics/bacterial number ratio in the DRB biofilm, helped explain the difference in the fouling degree between each group. Moreover, microbial community analysis showed that the relative abundance of typical highly secretory and biofouling-related genera, such as *Pseudomonas*, *Sphingomonas*, *Acinetobacter*, *Methylobacterium*, *Sphingobium*, and *Ralstonia*, were the main reasons for the difference in biofouling degree. All types of disinfection effectively prevented pathogen reproduction in the DRB biofilm. However, the relative abundance of (opportunistic) pathogens increased significantly after NaClO and ClO_2 disinfection.

1. Introduction

Water scarcity is a pressing global challenge [1]. The accelerated carbon neutrality process worsens water shortages [2,3]. Meanwhile, countries and regions continue to face water contamination [4]. Water reclamation is a win-win strategy for increasing freshwater supply and shortening the water footprint of human beings [5,6].

Reverse osmosis (RO) is one of the most applicable and stable units for high-quality reclaimed water production for industrial reuse, potable reuse, and groundwater replenishment [7–10]. Many large-scale water reclamation plants have been successively operated [11–13]. However, RO system has a fatal defect, that is, the unmanageable membrane fouling [14]. Membrane fouling of RO mainly includes scaling, colloidal fouling, organic fouling, and biofouling [15]. Among these, biofouling is the most complicated and uncontrollable, although numerous studies have made significant efforts to reduce it [16–19].

Disinfection is a widely applied pretreatment process used to deal with biofouling in RO systems. However, it may lead to undesirable effects [18]. After reducing the number of bacteria in the feed water, the disinfection process exerts a salient selection effect on the bacterial community and the extracellular polymeric substance (EPS) secreting ability of the bacteria. Some unwanted bacteria, that are resistant to disinfection or can adapt to adverse environments, might survive disinfection processes and become

disinfection-residual-bacteria (DRB) [20,21]. DRB might possess a higher proportion of bacteria with higher EPS secreting ability, leading to a more severe biofouling of RO membranes, especially in the long-term operation of RO systems [22]. Research in laboratory and full-scale water treatment plants has shown the probability of aggravated biofouling after disinfection [11,23–25]. However, most of these studies are limited to a single type of disinfection process [26]. To date, there is still a lack of systematic and broad comparison of the biofouling-control effects of various disinfection methods.

To provide more constructive and reliable guidance on the prevention of RO biofouling, this study compared the DRB characteristics of seven different disinfection methods, including five widely used disinfection methods (NaClO, NH_2Cl, ClO_2, UV, and O_3) and two novel disinfection methods (K_2FeO_4 and flow-through electrode system (FES) [27]) via a long-term (32 days) biofilm cultivation experiment on RO membranes. Furthermore, the bacteria and organic matter in the biofilm on the RO membranes were analysed using heterotrophic plate count (HPC), adenosine triphosphate (ATP), dissolved organic matter (DOM), and fluorescence excitation-emission matrix (EEM) to determine the primary reasons for the differences in biofouling in each group. The microbial community structure of DRB biofilms was analysed using high-throughput sequencing. Based on these results, the correlations between the fouling characteristics of DRB biofilms and bacterial density, organic density, biofilm morphology, and the microbial community of DRB were analysed.

2. Materials And Methods

2.1 Water samples

Reclaimed water was sampled from a large-scale water reclaimed plant in Beijing, China. A schematic of the advanced treatment process is shown in Fig. S1. The effluent from the denitrification filter was chosen as the sample because subsequent treatment units had a bacterial removal effect [28]. The reclaimed water samples were transported to the laboratory within 1 h, then filtered by filter papers to remove particles, and kept at 4°C before disinfection. Water quality parameters of the sampled water were measured as soon as they arrived at the laboratory, and are listed in Table 1.

Table 1
Chemical and physical properties of water samples before disinfection.

pH	TDS (mg/L)	TN (mg/L)	NO_3^- (mg/L)	NH_4^- (mg/L)	TP (mg/L)	TOC (mg/L)
7.8 ± 0.1	579 ± 27	13.2 ± 1.2	12.6 ± 1.4	0.38 ± 0.12	0.16 ± 0.02	5.84 ± 0.04

2.2 Disinfection and biofilm culture

Five commonly used disinfection methods, including NaClO, NH_2Cl, ClO_2, UV, and O_3, and two novel disinfection technologies, namely K_2FeO_4 and a flow-through electrode system (FES), were compared in this study. The steps followed in the experiment are shown in Fig. 1. Briefly, water samples were filtered

using filter paper (medium speed, Newstar, Hangzhou, China) to remove large flocs before disinfection. Seven types of disinfection processes were conducted by following the technical parameters described in preliminary experiments (Table 2) to achieve similar bacterial log removal, except for two novel disinfection methods as they could not achieve a high disinfection effect in actual wastewater. Square-wave alternating pulse current FES devices were set up based on a previous study [27]. The voltage amplitude and hydraulic retention time were set at 4 V and 27.7 s, respectively, to achieve the best disinfection performance of the system. UV irradiation was performed using a laboratory-scale collimated light-beam apparatus [24,29]. Other oxidizing disinfection processes were performed in sterilised glass bottles at 25°C and 150 rpm. The reaction was quenched with $Na_2S_2O_3$ solution to avoid oxidative damage to the RO membrane.

Table 2
Dosage of each disinfection method.

Disinfection method	Free chlorine	Chloramine	Chlorine dioxide	UV
Dosage	5 mg/L 30 min	5 mg/L 30 min	1 mg/L 30 min	30 mJ/cm^2
Disinfection method	Ozone	Ferret	FES	
Dosage	3 mg/L 10 min	5 mg/L 10 min	E = 4 V, T = 27.7 s	

Aromatic polyamide composite LP100 RO membrane (Vorton, China) was cut into round coupons (d = 32 mm, S = 804 mm^2), and the pretreatment procedure was conducted based on a previous study [30]. For biofilm culturing, the membrane coupon was soaked in 18 mL of disinfected water or control samples in a 5 cm sterilised round plastic Petri dish at 25°C. Water samples were refreshed daily. After 32 days of culture, the membrane was gently rinsed twice with phosphate buffer saline (PBS) to remove suspending bacteria for sequencing analysis. The experiments were conducted in triplicates for each group.

2.3 Evaluation of the disinfection effect

The disinfection effect was evaluated based on the concentration of culturable bacteria; ATP was tested before the biofilm culture experiments with triplicate experiments immediately after the disinfection processes were completed. Culturable bacteria were measured by HPC via colony-forming unit (CFU) counting [28]. ATP was tested using luminescence analysis. For total ATP measurement, 100 µL of the bacterial suspension and 100 µL of CellTiter-Glo Luminescent Cell Viability Assay (Promega, USA) were mixed in 96-well plates. After incubation at 25°C and at 150 rpm in the dark for 1 min, luminescence intensity was measured using a microplate reader (SpectraMax M5, Molecular Devices, USA). For the extracellular ATP test, water samples were filtered through a 0.1 µm membrane (Millipore) to remove bacteria; the subsequent steps were the same as those for total ATP. Intracellular ATP concentration was calculated by subtracting the extracellular ATP concentration from the total ATP concentration.

2.4 RO cross-flow unit and membrane performance tests

A laboratory-scale cross-flow RO system was used to evaluate the performance of RO membranes before and after biofilm growth [31]. Briefly, the membrane compaction phase was performed with a 30 min rinse of ultra-pure water at 1.2 MPa until the permeate flux was stable. The flow rate of the influent was set at 1.0 mL/min via a constant flow pump (NPL-100). The feed water was then switched to a 500 mg/L NaCl solution (conductivity of approximately 1000 μs/cm). The permeate flux was recorded after reaching a constant value. The normalised flux was calculated by dividing the flux of the fouled membrane by the clean membrane before biofilm growth.

The resistance of the RO membrane was calculated, as follows:

$$R_b = R_T - R_m - R_P = \frac{\Delta P}{\sigma J} R_m - R_P \quad (1)$$

Where, ΔP is the transmembrane pressure, σ is the kinetic viscosity of water, and J is the flux. The resistance of the biofilm R_b is calculated by subtracting the resistance of the virgin membrane R_m and the resistance of the concentration polarisation R_p from the resistance of the fouled membrane R_T.

2.5 Biofilm analysis

2.5.1 Heterotrophic plate counts (HPC) and microbial activity

Microbial amount and activity were determined using HPC and ATP concentrations. A piece of 10 mm×10 mm fouled membrane was cut off and vortexed in 0.5 mL normal saline for 30 s. HPC and ATP concentrations were tested using the same procedure, as described in Section 2.3.

2.5.2 Organic matter analysis

DOM and EEM were applied to reflect the characteristics of organic matter in DRB biofilms [23,32]. Briefly, a piece of 10 mm×10 mm fouled membrane was cut and shaken in 5 mL NaOH solution (pH 12) for 24 h at 25°C and 150 rpm. Then, HCl solution (pH 2) was added to adjust the pH of the solution to 7.0 ± 0.2. After neutralisation, the volume of the solution was adjusted to 15 mL by adding ultrapure water. The solution was filtered through a 0.45-μm nylon membrane (Whatman, England) before total organic carbon (TOC) measurement on a TOC-5000A analyser. EEM spectra were recorded using a fluorescence spectrophotometre (F-7100, Hitachi). The EEM spectrum was divided into six zones for integration. The types of fluorescent substances in each zone are shown in Table S1 [24,33].

2.5.3 Surface morphology of the fouled membrane

A laser scanning confocal microscope (LSCM, LSM710META) was used to measure the thickness of the biofilm on the RO membrane. A 5 ×10 mm membrane with the DRB biofilm of each sample was cut for LSCM observation. The staining groups of the fluorescent dyes and their targets are listed in Table S2.

The surface morphology of the DRB biofilm was examined using field-emission scanning electron microscopy (FESEM, SU8220, Hitachi, Japan) and the accelerating voltage was set to 5 kV. A piece of 5 × 5 mm membrane coupons was cut for observation.

2.5.4 Microbial community analysis

Three pieces of 40 mm^2 membrane coupons were cut for microbial community analysis. Microbial community analysis was conducted as previously described [23]. Briefly, DNA was extracted using the E.Z.N.A.® soil DNA Kit (Omega Bio-Tek, Norcross, GA, U.S.). Furthermore, 338F (5'-ACTCCTACGGGAGGCAGCAG-3') and 806R (5'-GGACTACHVGGGTWTCTAAT-3') were used as primer pairs for amplification. Sequencing was performed using an Illumina MiSeq PE300 platform. All analysed sequences were submitted to the NCBI SRA database under accession number PRJNA803872. Pathogen identification was based on the Virulence Factor Database (VFDB) from the Institute of Pathogen Biology, CAMS & PUMC.

3. Results And Discussion

3.1 Effects of DRB biofilm on the RO membrane performance

The effects of different disinfection methods on the RO membrane flux of the DRB biofilms were investigated. Not all disinfection methods can control biofouling. These methods were divided into three groups, according to the normalised flux (Fig. 2a). The first group, classified as “alleviated”, included K_2FeO_4 and O_3. Their DRB performed light normalised flux drop (22.4 ± 2.4% and 23.9 ± 1.17%, respectively) compared to the control group (without disinfection pre-treatment), thereby indicating alleviated biofouling potentials. Meanwhile, the DRB of NH_2Cl had a similar biofouling degree as the control group (~ 27%), and was classified as “equal”. Finally, the DRB of the “aggravated” group, which included FES, UV, NaClO, and ClO_2, caused more biofouling of the RO membrane than the control group. Notably, the biofouling of ClO_2-DRB was the most severe, with a flux drop percentage of 35.5 ± 4.0%. The two most frequently used disinfection methods, namely UV and NaClO significantly aggravated the biofouling of RO membranes, matching the results of long-term studies in previous research [23,24].

The hydraulic resistance of the DRB biofilms (*Rm*) is shown in Fig. 2b. The resistance of the K_2FeO_4-DRB biofilm (2.48×10^{13} m^{-1}) was the lowest as it had the least impact on the RO membrane flux drop. Also, the resistance of the O_3-DRB biofilm (2.71×10^{13} m^{-1}) in the “alleviated” group was lower than that of the control group (3.07×10^{13} m^{-1}). The resistance of the NH_2Cl-DRB biofilm (3.48×10^{13} m^{-1}) was slightly higher than that of the control group. The DRB biofilm resistance of all the “aggravated” groups was much higher than that of the control group. Among them, the average resistance of NaClO was the highest, at 5.18×10^{13} m^{-1}. However, it had a relatively high within-group error, corresponding to the membrane flux drop shown in Fig. 2a.

3.2 Disinfection effect of seven kinds of disinfection methods

Alleviation of biofouling after disinfection might be associated with lower bacterial concentrations in the feed water after disinfection [23]. Therefore, variations in the concentrations of HPC and ATP in the water samples during the disinfection processes were tested (Table 3). The five conventional disinfection methods achieved a bacterial inactivation rate of 3-lg, while K_2FeO_4 and FES exhibited a relatively low inactivation effect (~ 1-lg). Overall, HPC had no monotonous correlation with biofouling potential. The DRB biofilm of K_2FeO_4 caused only a 22% decrease in membrane flux, although the inactivation effect of K_2FeO_4 was the lowest (< 1-lg). NaClO was the most effective method for bacterial inactivation. However, its DRB aggravated biofouling at an average relative flux drop of ~ 35%.

Table 3
Disinfection effect measured by HPC and ATP content.

Disinfection methods	HPC (CFU/mL)	Inactivation rate (lg)	ATP (ng/mL) (Total)	ATP (ng/mL) (Intracellular)
Control	2.7 ± 0.1*10^5	--	2.99 ± 0.08	2.90 ± 0.08
K_2FeO_4	2.4 ± 0.2*10^4	1.06 ± 0.05	0.65 ± 0.01	0.61 ± 0.00
O_3	1.5 ± 0.5*10^2	3.28 ± 0.14	2.93 ± 0.18	0.11 ± 0.01
NH_2Cl	4.3 ± 2.3*10^1	3.88 ± 0.25	0.24 ± 0.02	0.18 ± 0.02
FES	1.6 ± 0.1*10^4	1.23 ± 0.04	0.61 ± 0.02	0.35 ± 0.00
UV	2.5 ± 0.8*10^2	3.06 ± 0.15	5.11 ± 0.24	4.92 ± 0.23
NaClO	3.0 ± 1.0*10^1	3.98 ± 0.14	4.03 ± 0.12	0.21 ± 0.01
ClO_2	1.5 ± 0.1*10^2	3.27 ± 0.01	0.59 ± 0.02	0.45 ± 0.02

Previous studies have reported that ATP can be an effective indicator for predicting biofouling potentials in the short- or medium-term operation of RO systems (less than 16 days) [15,34]. However, this conclusion is not valid in long-term experiments (Table 3). The intracellular ATP in the control group was 2.90 ng/mL, accounting for 97% of the total ATP. Total and intracellular ATP concentrations increased after UV treatment, partly because of the rapid DNA repair mechanism triggered by UV radiation. No correlation was found between the DRB biofouling potentials (membrane flux drop) and the ATP concentration of DRB. Evaluation of the disinfection effect suggested that the amount and the activity of DRB were not the decisive factors of biofouling potential during long-term operation.

3.3 Characteristics of the DRB biofilm on RO membranes

To determine the reasons for varying performances of RO membranes fouled by different DRB biofilms, this study dissected the fouled RO membranes and performed a series of tests. The number of bacteria and organics in the DRB biofilms, the morphological characteristics of DRB biofilms, and the bacterial community structure were analysed.

3.3.1 Bacteria and dissolved organic matters (DOM) in the DRB biofilms

The live bacterial density of the DRB biofilm was measured using HPC, as shown in Fig. 3a. DRB biofilms of NH_2Cl, FES, and UV possessed the maximum live bacteria density (approximately 10^6 CFU/cm^2). The live bacterial density of NaClO- and ClO_2-DRB biofilms were lower than that of the control group (approximately 10^5 CFU/cm^2), but they led to the worst flux drop in the RO membrane. Hence, the live bacterial density of the DRB biofilm was not a key factor leading to differences in biofouling degrees. This conclusion is consistent with previous studies [24].

Unlike bacterial cells, the extracellular polymeric substances (EPS) on RO membranes have a more direct relationship with flux drop [31,35]. Hence, the total amount of organics in the DRB biofilms was measured by DOM (Fig. 4a), and the different component of DOM was tested using EEM (Fig. S2). The amount of DOM did not show a clear correlation with the biofouling degree. The DOM of K_2FeO_4, which was in the “alleviated” group, was much higher than that of the “aggravated” group. Therefore, the total amount of organics did not play a key factor in the degree of DRB biofilm fouling.

Considering that the ratio of EPS to bacteria could affect the biofouling degree [35], this study calculated the ratio of DOM to HPC in the DRB biofilms (Fig. 4b). The DOM/HPC ratio in the control group was approximately 4 mg/10^7 live cells. The DRB biofilm of K_2FeO_4, O_3, NH_2Cl, FES, and UV possessed a relatively lower DOM/HPC ratio, while those of NaClO and ClO_2 (5.4 and 7.6 mg/10^7 live cell, respectively) were significantly higher than the control group. This implied that these two disinfectants could aggravate biofouling of the RO membrane by reshaping the microbial community and changing the EPS production capacity of the residual bacteria.

The proportions of DOM components among all the groups were similar (Fig. S2). Tyrosine/tryptophan amide (Zone) and protein-containing tyrosine/tryptophan (Zone II) were the dominant components of fluorescent organic matter in each DRB biofilm, indicating that amino acids and proteins were predominant in the DRB biofilms, compared with polysaccharides, fulvic acids, or humid acids.

3.3.2 Morphological characteristics of DRB biofilms

Compared to the bacterial and organic densities in the biofilm, the degree of biofouling was more closely correlated with the thickness and consecutiveness of the biofilm on RO membranes. The thickness of the DRB biofilm was tested using z-stack images of the LSCM. The surface image of the DRB biofilm showed that bacteria, proteins, and α-/β-polysaccharides were evenly distributed in the DRB biofilm (Fig. S3). The

DRB biofilm of K_2FeO_4 was relatively loose in section view, while the others were consecutive (Fig. 5). The average thickness of the DRB biofilm was measured via cross-section (Fig. S4) and is shown in Fig. 5. As a result, the DRB biofilm of the UV group (55 ± 1μm) was significantly thicker than that of the control group (33 ± 1μm). The DRB biofilm thickness of the “alleviated” group was approximately 22 μm, which was the lowest of all the groups. The biofilm thickness partly illustrated the difference in the biofouling degree, supplemented by the DOM/HPC ratio. The two disinfection methods in the “alleviated” group caused a low DOM/HPC ratio and thinner biofilm on the RO membrane, leading to a marginal flux drop of the fouled membrane. The UV DRB developed a thick biofilm and led to severe biofouling of the RO membrane. The biofilms of NaClO and ClO_2 were not very thick. However, the high DOM/HPC ratio in the biofilm could narrow the water channels between bacterial cells [35], leading to the highest flux drop in the RO membrane.

The FESEM images of the DRB biofilm are shown in Fig. 6. The DRB biofilm fully covered all the RO membranes. However, the compactness of the biofilms was different. The UV and NaClO-DRB biofilms were compact and continuous, partly illustrating their severe biofouling performance. In contrast, there were gaps between the bacteria and the EPS matrix in the DRB biofilm of the remaining groups. Regular crystals containing Fe were observed in the K_2FeO_4 group (Fig. S5), indicating that K_2FeO_4 could cause scaling of the RO membrane.

3.4 Microbial community analysis of DRB biofilm on RO membranes

Disinfection processes can exert three levels of change on the bacteria: metabolic change of a single bacteria, shift in the microbial community, and variation of nutrient conditions [20]. Among them, a shift in the microbial community is most likely to affect the biofouling degree during long-term operations [36]. Therefore, we analysed the alpha and beta diversities of the DRB microbial community.

The alpha diversity indices of the observed species as well as the ACE, Chao1, and Shannon indices of bacteria in the DRB biofilm are listed in Table 4. The community richness and evenness of the control group were the highest, followed by K_2FeO_4 (“alleviated” group), which has been reported to have minimal impact on the bacterial community [37]. The community evenness of the ClO_2-DRB biofilm (“aggravated” group) was the lowest, indicating a significant selection effect of ClO_2. Overall, community richness and evenness did not show a monotonous correlation with the biofouling behaviour of DRB biofilms.

Table 4
Statistical table of Alpha diversity index.

Disinfection methods	Observed species	ACE	Chao1	Shannon	Simpson
Control	864.7 ± 4.9	1004.9 ± 22.7	1004.1 ± 34.8	4.19 ± 0.08	0.052 ± 0.005
K_2FeO_4	445.7 ± 4.5	539.9 ± 18.4	544.0 ± 29.4	3.75 ± 0.05	0.066 ± 0.003
O_3	135.3 ± 0.5	184.3 ± 9.7	166.0 ± 9.6	2.69 ± 0.00	0.146 ± 0.002
NH_2Cl	164.3 ± 26.7	307.8 ± 119.2	230.6 ± 66.0	2.46 ± 0.04	0.132 ± 0.013
FES	296.0 ± 3.7	459.3 ± 65.0	399.8 ± 22.8	2.45 ± 0.08	0.286 ± 0.019
UV	221.3 ± 1.7	464.1 ± 63.7	327.5 ± 29.1	2.82 ± 0.05	0.119 ± 0.006
NaClO	261.3 ± 25.0	283.1 ± 20.6	283.7 ± 17.7	2.39 ± 0.15	0.240 ± 0.010
ClO_2	94.3 ± 6.9	167.2 ± 82.9	125.2 ± 37.3	2.00 ± 0.04	0.191 ± 0.009

A Venn diagram of the OTUs that appeared in each group is shown in Fig. S6. Only 36 OTUs were shared by all the groups. The control group had the highest OTUs, indicating that each disinfection method had a selection effect. Besides the control group, the number of OTUs in the K_2FeO_4-DRB biofilm was the highest. High numbers of OTUs caused fierce competition among the species, and inhibited biofilm growth and EPS secreting, resulting in the least biofouling of the K_2FeO_4-DRB biofilm. The DRB biofilm with ClO_2 and O_3 disinfection possessed the lowest OTUs, indicating that the two aforementioned oxidising disinfection methods had strong selectivity for the bacteria [38]. However, as their biofouling performance differed, ClO_2 selected more biofilm formation and EPS-secreting species than O_3.

The microbial community structure at the phylum level is shown in Fig. S7a; class and genus levels are shown in Fig. S8. α-Proteobacteria and γ-Proteobacteria were the dominant classes in all the DRB biofilms. Actinobacteria and Bacteroidetes were the second and third most abundant phyla, respectively. The top three phyla accounted for 90% of all bacteria. A heat map at the genus level is shown in Fig. S7b.

Previously reported biofouling-related genera had significantly higher relative abundances in the “aggravated” group, namely, ClO_2, NaClO, UV, and FES. For instance, *Methylobacterium*, which is a typical disinfection-resistant and biofouling-related bacteria genus [23,35], was dominant in the DRB biofilm of FES and ClO_2 with a relative abundance of 54.8 ± 2.3% and 28.6 ± 1.7%, respectively. *Sphingobium*, a highly secretory genus [24,39], was found to dominate the DRB biofilm under UV (30.0 ± 0.8%). In addition, the

relative abundance of *Pseudomonas* was significantly higher in the NaClO-DRB biofilm than in the other groups (45.9 ± 1.8%). *Pseudomonas*, which is a typical DRB of chlorine [20] causes biofouling of RO membranes [23,40–42]. In contrast, the relative abundance of these genera was significantly lower in the K_2FeO_4-and O_3-DRB biofilms (< 10%). Thus, the relative abundance of highly secretory or biofouling-related genera plays a decisive role in the biofouling potential of DRB during long-term operation.

A community structure similarity analysis was performed using the PCA algorithm (Fig. 7). The community structures of all the disinfection groups were significantly different from those of the control group. The bacterial community structures of UV-, O_3-, NH_2Cl-, NaClO-, and K_2FeO_4-DRB biofilms were similar, whereas the community structures of ClO_2 and FES DRB biofilms were similar. This may be the cause of the inability of these two disinfectants to control the highly secretory genus *Methylobacterium*.

Apart from biofouling of RO membranes, the DRB biofilm can act as a shelter for pathogenic bacteria, leading to health risks of RO concentrate [43]. Thus, the cumulative abundance of pathogens and opportunistic pathogens in the DRB biofilm was analysed and shown in Fig. S9. The relative abundance of pathogenic bacteria in the DRB biofilm increased significantly after disinfection with NaClO and ClO_2, indicating that these two chlorine-containing oxidative disinfectants selected (opportunistic) pathogens. K_2FeO_4, FES, and NH_2Cl partially reduced the relative abundance of (opportunistic) pathogens. Furthermore, their abundance in DRB biofilms of O_3 and UV were the lowest, demonstrating that they controlled the spread of (opportunistic) pathogens in biofilms.

3.5 Correlation between microbial community structure and RO membrane flux

To identify the key genera in the microbial community of DRB affecting the RO membrane flux, correlation coefficients between the normalised flux and relative abundance of the top 50 genera in all the experimental groups and the control group are shown in Fig. 8. The relative abundance of *Methylobacterium* (a typical disinfection-resistance and biofouling-related genus [23,35]) was negatively correlated with the normalised flux of the fouled RO membrane ($p < 0.05$). The relative abundances of two kinds of high EPS-secreting bacteria, *Microbacterium* and *Pseudomonas*, were also negatively correlated with the normalised flux. These two genera consist of typical chlorine-resistant and highly secretory bacteria. Hence, *Methylobacterium*, *Microbacterium*, and *Pseudomonas* deserve special attention as they play an essential role in the aggravated biofouling potential after disinfection.

Additionally, we calculated the accumulative relative abundance of typical highly secretory or biofouling-related genera reported in the literature, including *Pseudomonas*, *Sphingomonas*, *Acinetobacter*, *Methylobacterium*, *Sphingobium*, and *Ralstonia* [23–25, 39,40,44] (Fig. 9). The cumulative relative abundance of these bacteria in the “aggravated” group, namely the FES, UV-, NaClO-, and ClO_2- DRB biofilms was significantly higher than that in the control group (~ 5%). Remarkably, the highly secretory bacteria accounted for over half of the total bacteria in the DRB biofilms of FES and NaClO, that is 56.4% and 53.0%, respectively.

In contrast, the DRB biofilm of the “alleviated” group possessed a similar proportion of highly secretory bacteria as that of the control group. The decrease in bacterial numbers after disinfection could explain biofouling alleviation. Therefore, variation in the relative abundance of typical highly secretory and biofouling-related genera was the main reason for the change in biofouling potentials after different disinfection processes.

4. Conclusions

In the long-term experiment (32 days), K_2FeO_4 and O_3 alleviated biofouling of the DRB biofilm. Biofouling degree of the NH_2Cl-DRB biofilm was similar to that of the control group, whereas the other four types of disinfection aggravated membrane biofouling. Furthermore, as ferrate introduced iron flocs and aggravated inorganic scaling in RO systems, O_3 was recommended as a practical approach to prevent biofouling in RO systems.

Morphological analysis combined with the DOM/HPC ratio explained the difference in the fouling behaviour of the DRB biofilms. A high DOM/HPC ratio along with denser and thicker DRB biofilms led to severe biofouling.

Community analysis revealed that the selection effect of disinfection on typical highly secretory and biofouling-related genera was the primary reason for biofouling aggravation. Typical genera included *Pseudomonas*, *Sphingomonas*, *Acinetobacter*, *Methylobacterium*, *Sphingobium*, and *Ralstonia*.

Declarations

Acknowledgements

This study was supported by the Key Program of the National Natural Science Foundation of China (No. 51738005) and the National Natural Science Foundation of China (No. 52000114).

Competing interests

We declare that we have no financial and personal relationships with other people or organizations that can inappropriately influence our work, and there is no professional or other personal interest of any nature or kind in any product, service and/or company that could be construed as influencing the position presented in, or the review of, the manuscript entitled.

Author Contributions

Hao-Bin Wang: Conceptualization, Methodology, Original draft preparation. **Yin-Hu Wu**: Writing- Reviewing and Editing, Project administration, Funding acquisition, Supervision. **Wen-Long Wang**: Writing- Reviewing

and Editing. **Li-Wei Luo**: Conceptualization. **Gen-Qiang Chen**: Conceptualization. **Zhuo Chen**: Writing- Reviewing and Editing Writing. **Song Xue**: Formal analysis. **Ao Xu**: Writing- Reviewing. **Yu-Qing Xu**: Investigation. **Nozomu Ikuno**: Writing- Reviewing and Resource. **Kazuki Ishii**: Resource. **Hong-Ying Hu**: Project administration, Supervision.

Data Availability

DNA sequences are available at the NCBI Sequence Read Archive, accession number: PRJNA803872.

References

1. Gleick, P. H. & Cooley, H. Freshwater Scarcity. *Annual Review of Environment and Resources* **46**, 319-348, doi:10.1146/annurev-environ-012220-101319 (2021).
2. Ding, N., Liu, J., Yang, J. & Lu, B. Water footprints of energy sources in China: Exploring options to improve water efficiency. *Journal of Cleaner Production* **174**, 1021-1031, doi:https://doi.org/10.1016/j.jclepro.2017.10.273 (2018).
3. Qin, Y. Global competing water uses for food and energy. *Environmental Research Letters* **16**, doi:10.1088/1748-9326/ac06fa (2021).
4. Xu, A. *et al.* Towards the new era of wastewater treatment of China: Development history, current status, and future directions. *Water Cycle* **1**, 80-87, doi:https://doi.org/10.1016/j.watcyc.2020.06.004 (2020).
5. Wencki, K. *et al.* Approaches for the evaluation of future-oriented technologies and concepts in the field of water reuse and desalination. *Journal of Water Reuse and Desalination* **10**, 269-283, doi:10.2166/wrd.2020.022 (2020).
6. Takeuchi, H. & Tanaka, H. Water reuse and recycling in Japan — History, current situation, and future perspectives. *Water Cycle* **1**, 1-12, doi:https://doi.org/10.1016/j.watcyc.2020.05.001 (2020).
7. Page, D. *et al.* Progress in the development of risk-based guidelines to support managed aquifer recharge for agriculture in Chile. *Water Cycle* **1**, 136-145, doi:https://doi.org/10.1016/j.watcyc.2020.09.003 (2020).
8. Farhat, N. M. *et al.* Application of monochloramine for wastewater reuse: Effect on biostability during transport and biofouling in RO membranes. *Journal of Membrane Science* **551**, 243-253, doi:10.1016/j.memsci.2018.01.060 (2018).
9. Tong, X. *et al.* Fouling properties of reverse osmosis membranes along the feed channel in an industrial-scale system for wastewater reclamation. *Sci. Total Environ.* **713**, 136673, doi:https://doi.org/10.1016/j.scitotenv.2020.136673 (2020).
10. Tseng, S.-f., Lo, C.-M. & Hung, C.-h. Evaluation of the benefit of practically operating reverse osmosis system in the factory: taking the recycling of KI solution and water of the screen polarizing plate as

an example. *Journal of Water Reuse and Desalination* **11**, 329-346, doi:10.2166/wrd.2021.110 (2021).

11. Luo, L.-W. *et al.* Aggravated biofouling caused by chlorine disinfection in a pilot-scale reverse osmosis treatment system of municipal wastewater. *Journal of Water Reuse and Desalination* **11**, 201-211, doi:10.2166/wrd.2021.108 %J Journal of Water Reuse and Desalination (2021).
12. Bai, Y. *et al.* Long-term performance and economic evaluation of full-scale MF and RO process – A case study of the changi NEWater Project Phase 2 in Singapore. *Water Cycle* **1**, 128-135, doi:https://doi.org/10.1016/j.watcyc.2020.09.001 (2020).
13. Yu, T. *et al.* Microcoagulation improved the performance of the UF–RO system treating the effluent from a coastal municipal wastewater treatment plant: a pilot-scale study. *Journal of Water Reuse and Desalination* **11**, 177-188, doi:10.2166/wrd.2021.099 (2021).
14. Qasim, M., Badrelzaman, M., Darwish, N. N., Darwish, N. A. & Hilal, N. Reverse osmosis desalination: A state-of-the-art review. *Desalination* **459**, 59-104, doi:10.1016/j.desal.2019.02.008 (2019).
15. Sim, L. N. *et al.* A review of fouling indices and monitoring techniques for reverse osmosis. *Desalination* **434**, 169-188, doi:10.1016/j.desal.2017.12.009 (2018).
16. Jahan Sajib, M. S. *et al.* Atomistic Simulations of Biofouling and Molecular Transfer of a Cross-linked Aromatic Polyamide Membrane for Desalination. *Langmuir* **36**, 7658-7668, doi:10.1021/acs.langmuir.0c01308 (2020).
17. Weinrich, L., LeChevallier, M. & Haas, C. N. Contribution of assimilable organic carbon to biological fouling in seawater reverse osmosis membrane treatment. *Water Res.* **101**, 203-213, doi:10.1016/j.watres.2016.05.075 (2016).
18. Al-Abri, M. *et al.* Chlorination disadvantages and alternative routes for biofouling control in reverse osmosis desalination. *NPJ Clean Water* **2**, 2, doi:10.1038/s41545-018-0024-8 (2019).
19. Abushaban, A. *et al.* Biofouling potential indicators to assess pretreatment and mitigate biofouling in SWRO membranes: A short review. *Desalination* **527**, 115543, doi:https://doi.org/10.1016/j.desal.2021.115543 (2022).
20. Wang, H.-B. *et al.* Risks, characteristics, and control strategies of disinfection-residual-bacteria (DRB) from the perspective of microbial community structure. *Water Res.* **204**, 117606, doi:https://doi.org/10.1016/j.watres.2021.117606 (2021).
21. Nordholt, N., Kanaris, O., Schmidt, S. B. I. & Schreiber, F. Persistence against benzalkonium chloride promotes rapid evolution of tolerance during periodic disinfection. *Nature Communications* **12**, 6792, doi:10.1038/s41467-021-27019-8 (2021).
22. Wang, Y.-H. *et al.* Metagenomics analysis of the key functional genes related to biofouling aggravation of reverse osmosis membranes after chlorine disinfection. *Journal of Hazardous Materials* **410**, 124602, doi:https://doi.org/10.1016/j.jhazmat.2020.124602 (2021).
23. Wang, Y.-H. *et al.* Chlorine disinfection significantly aggravated the biofouling of reverse osmosis membrane used for municipal wastewater reclamation. *Water Res.* **154**, 246-257, doi:https://doi.org/10.1016/j.watres.2019.02.008 (2019).

24. Wu, Y.-H. *et al.* Effect of ultraviolet disinfection on the fouling of reverse osmosis membranes for municipal wastewater reclamation. *Water Res.* **195**, 116995, doi:https://doi.org/10.1016/j.watres.2021.116995 (2021).
25. Khan, M. T., Hong, P.-Y., Nada, N. & Croue, J. P. Does chlorination of seawater reverse osmosis membranes control biofouling? *Water Res.* **78**, 84-97, doi:https://doi.org/10.1016/j.watres.2015.03.029 (2015).
26. Xuehao Zhao, Y. W., Xue Zhang, Xin Tong, Tong Yu, Yunhong Wang, Nozomu Ikuno, Kazuki Ishii, Hongying Hu. Ozonation as an efficient pretreatment method to alleviate reverse osmosis membrane fouling caused by complexes of humic acid and calcium ion. *Frontiers of Environmental Science & Engineering* **13**, 55-, doi:10.1007/s11783-019-1139-y (2019).
27. Ni, X.-Y. *et al.* Enhancing disinfection performance of the carbon fiber-based flow-through electrode system (FES) by alternating pulse current (APC) with low-frequency square wave. *Chemical Engineering Journal* **410**, 128399, doi:https://doi.org/10.1016/j.cej.2020.128399 (2021).
28. Cui, Q. *et al.* Bacterial removal performance and community changes during advanced treatment process: A case study at a full-scale water reclamation plant. *Sci. Total Environ.* **705**, 8, doi:10.1016/j.scitotenv.2019.135811 (2020).
29. Pullerits, K. *et al.* Impact of UV irradiation at full scale on bacterial communities in drinking water. *NPJ Clean Water* **3**, 10, doi:10.1038/s41545-020-0057-7 (2020).
30. Tong, X. *et al.* Simulating and predicting the flux change of reverse osmosis membranes over time during wastewater reclamation caused by organic fouling. *Environment International* **140**, 105744, doi:https://doi.org/10.1016/j.envint.2020.105744 (2020).
31. Chen, G.-Q. *et al.* Enhanced extracellular polymeric substances production and aggravated membrane fouling potential caused by different disinfection treatment. *Journal of Membrane Science* **642**, 120007, doi:https://doi.org/10.1016/j.memsci.2021.120007 (2022).
32. Mao, Y. *et al.* Characterization of bacterial fluorescence: insight into rapid detection of bacteria in water. *Journal of Water Reuse and Desalination*, doi:10.2166/wrd.2021.040 (2021).
33. Wang, Z.-P. & Zhang, T. Characterization of soluble microbial products (SMP) under stressful conditions. *Water Res.* **44**, 5499-5509, doi:https://doi.org/10.1016/j.watres.2010.06.067 (2010).
34. Weinrich, L., Haas, C. N. & LeChevallier, M. W. Recent advances in measuring and modeling reverse osmosis membrane fouling in seawater desalination: a review. *Journal of Water Reuse and Desalination* **3**, 85-101, doi:10.2166/wrd.2013.056 (2013).
35. Luo, L.-W. *et al.* Chlorine-resistant bacteria (CRB) in the reverse osmosis system for wastewater reclamation: isolation, identification and membrane fouling mechanisms. *Water Res.*, 117966, doi:https://doi.org/10.1016/j.watres.2021.117966 (2021).
36. Podar, M. *et al.* Microbial diversity analysis of two full-scale seawater desalination treatment trains provides insights into detrimental biofilm formation. *Journal of Membrane Science Letters* **1**, 100001, doi:https://doi.org/10.1016/j.memlet.2021.100001 (2021).

37. Li, C. *et al.* Bacterial community structure and microorganism inactivation following water treatment with ferrate(VI) or chlorine. *Environmental Chemistry Letters* **15**, 525-530, doi:10.1007/s10311-017-0623-5 (2017).
38. Proctor, C. R. & Hammes, F. Drinking water microbiology—from measurement to management. *Current Opinion in Biotechnology* **33**, 87-94, doi:https://doi.org/10.1016/j.copbio.2014.12.014 (2015).
39. Zhang, Y. *et al.* Extracellular polymeric substances enhanced mass transfer of polycyclic aromatic hydrocarbons in the two-liquid-phase system for biodegradation. *Appl. Microbiol. Biotechnol.* **90**, 1063-1071, doi:10.1007/s00253-011-3134-5 (2011).
40. Freitas, F., Alves, V. D. & Reis, M. A. M. Advances in bacterial exopolysaccharides: from production to biotechnological applications. *Trends in Biotechnology* **29**, 388-398, doi:https://doi.org/10.1016/j.tibtech.2011.03.008 (2011).
41. Wei, L. *et al.* Prevalence, Virulence, Antimicrobial Resistance, and Molecular Characterization of Pseudomonas aeruginosa Isolates From Drinking Water in China. *Frontiers in Microbiology* **11**, 2984 (2020).
42. Luo, L.-W. *et al.* Evaluating method and potential risks of chlorine-resistant bacteria (CRB): A review. *Water Res.* **188**, 116474, doi:https://doi.org/10.1016/j.watres.2020.116474 (2021).
43. Flemming, H.-C. *et al.* Biofilms: an emergent form of bacterial life. *Nat. Rev. Microbiol.* **14**, 563-575, doi:10.1038/nrmicro.2016.94 (2016).
44. Jung, J. & Park, W. Acinetobacter species as model microorganisms in environmental microbiology: current state and perspectives. *Appl. Microbiol. Biotechnol.* **99**, 2533-2548, doi:10.1007/s00253-015-6439-y (2015).

Figures

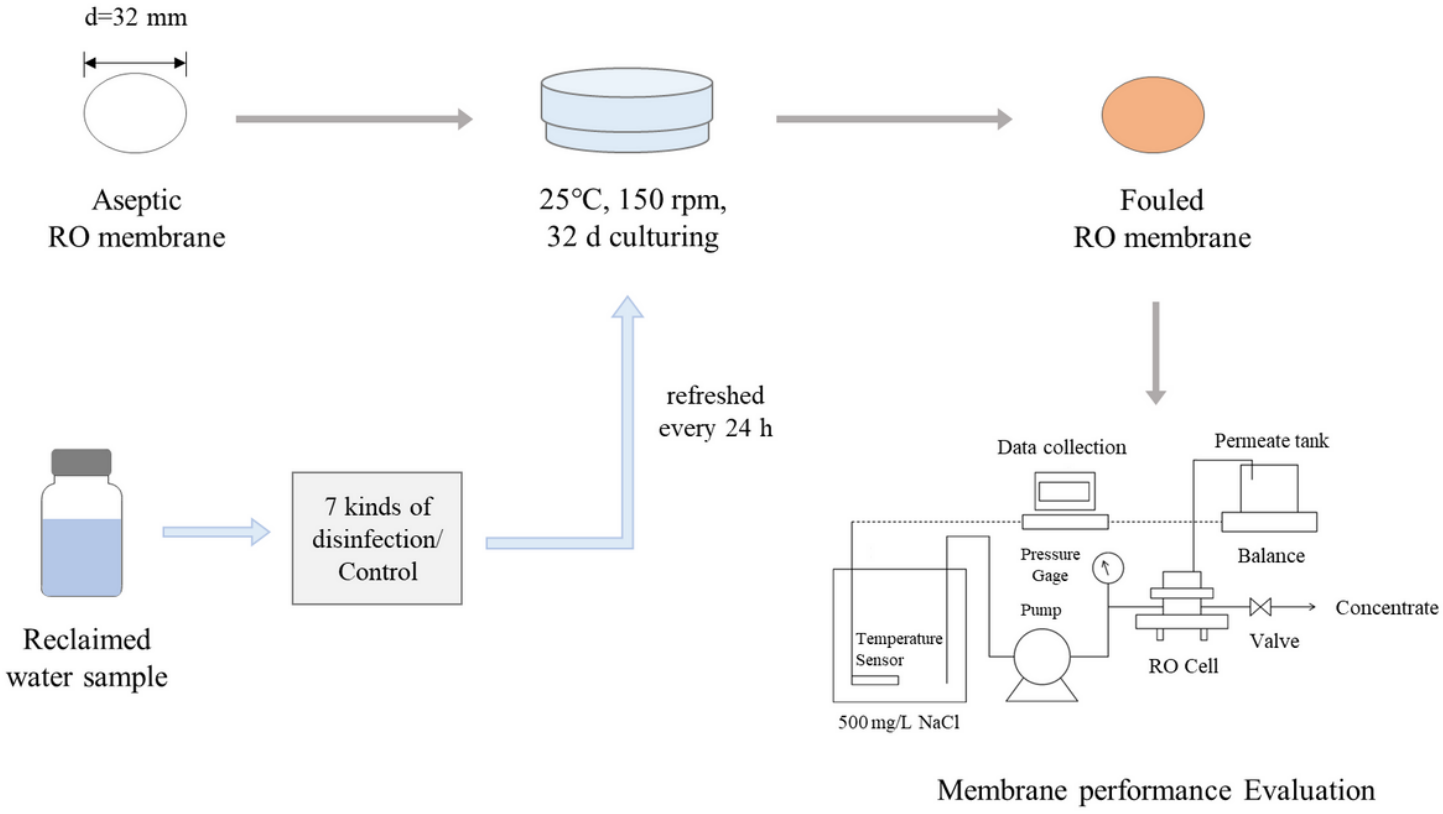

Figure 1

Schematic representation of the experimental procedure.

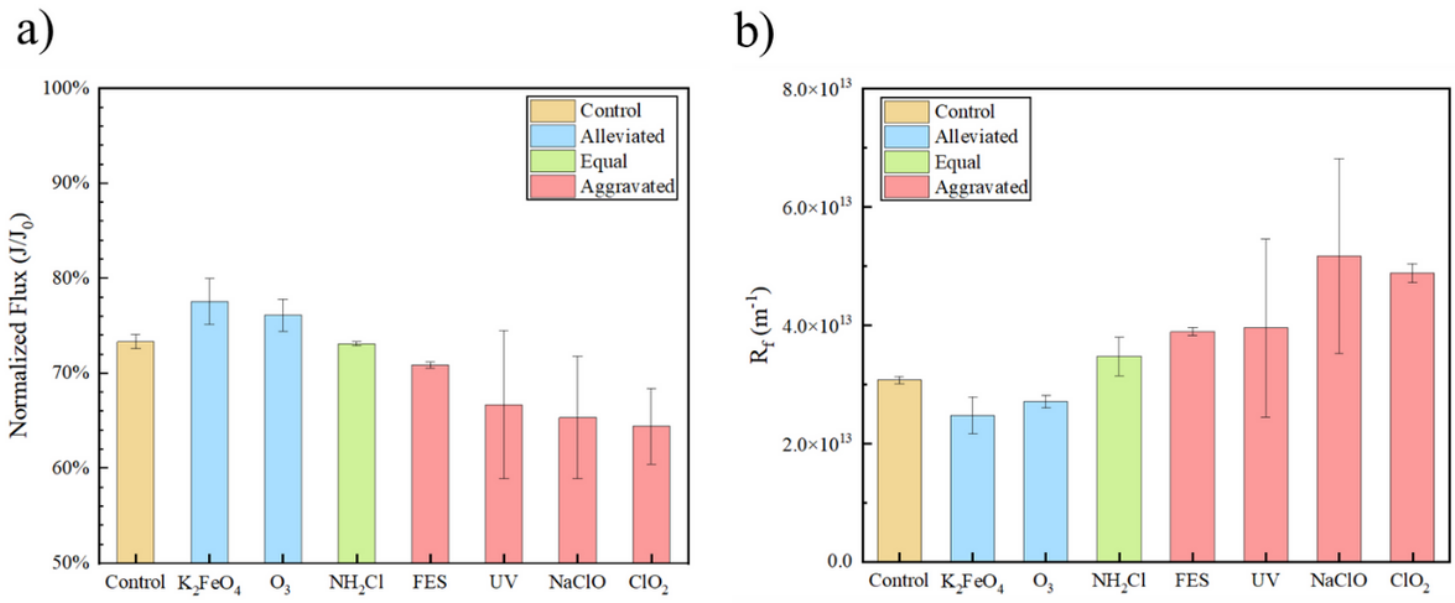

Figure 2

Normalised flux (a) and biofouling layer resistance (b) of RO membranes with DRB biofilm after seven different kinds of disinfection treatment.

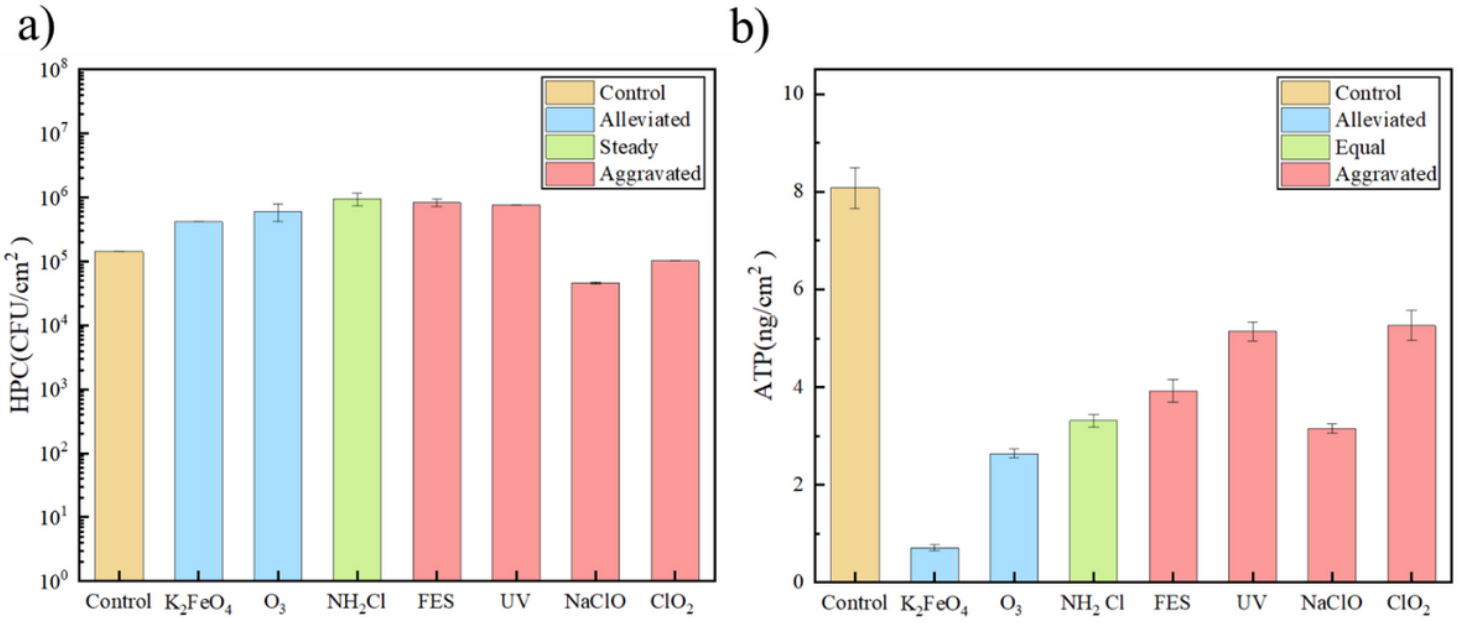

Figure 3

Culturable bacteria and ATP content of DRB biofilm on the surface of RO membranes.

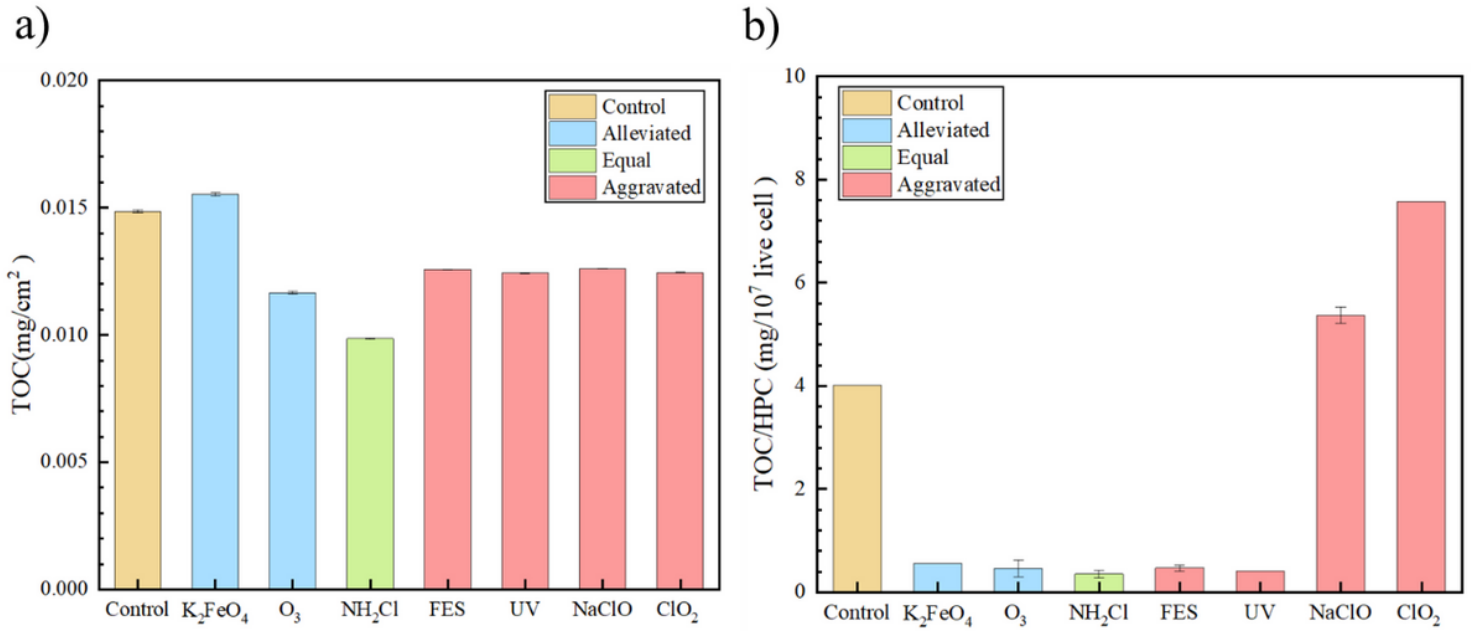

Figure 4

DOM and the ratio of DOM to HPC in the DRB biofilms.

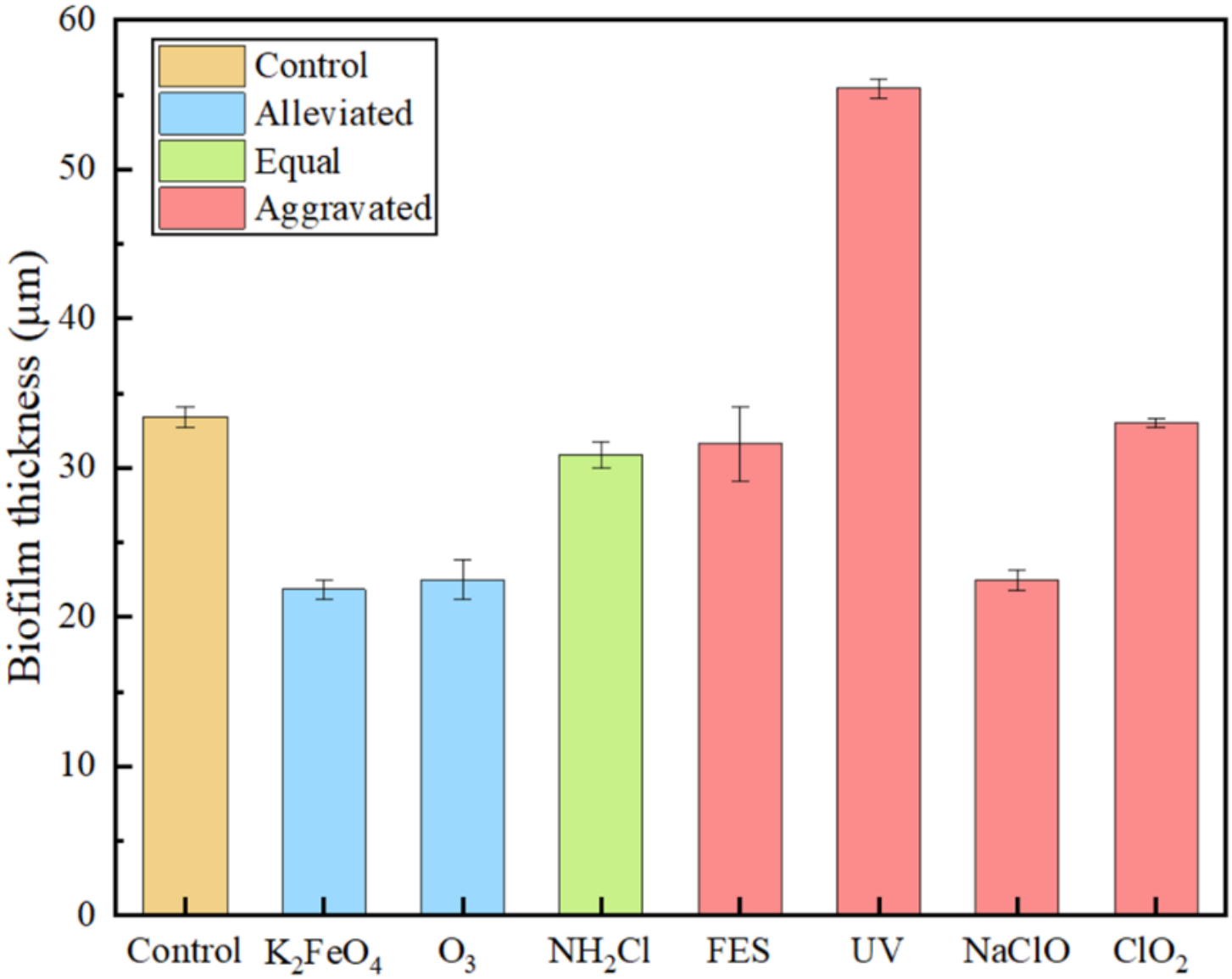

Figure 5

Thickness of DRB biofilms measured with laser scanning confocal microscope (LSCM).

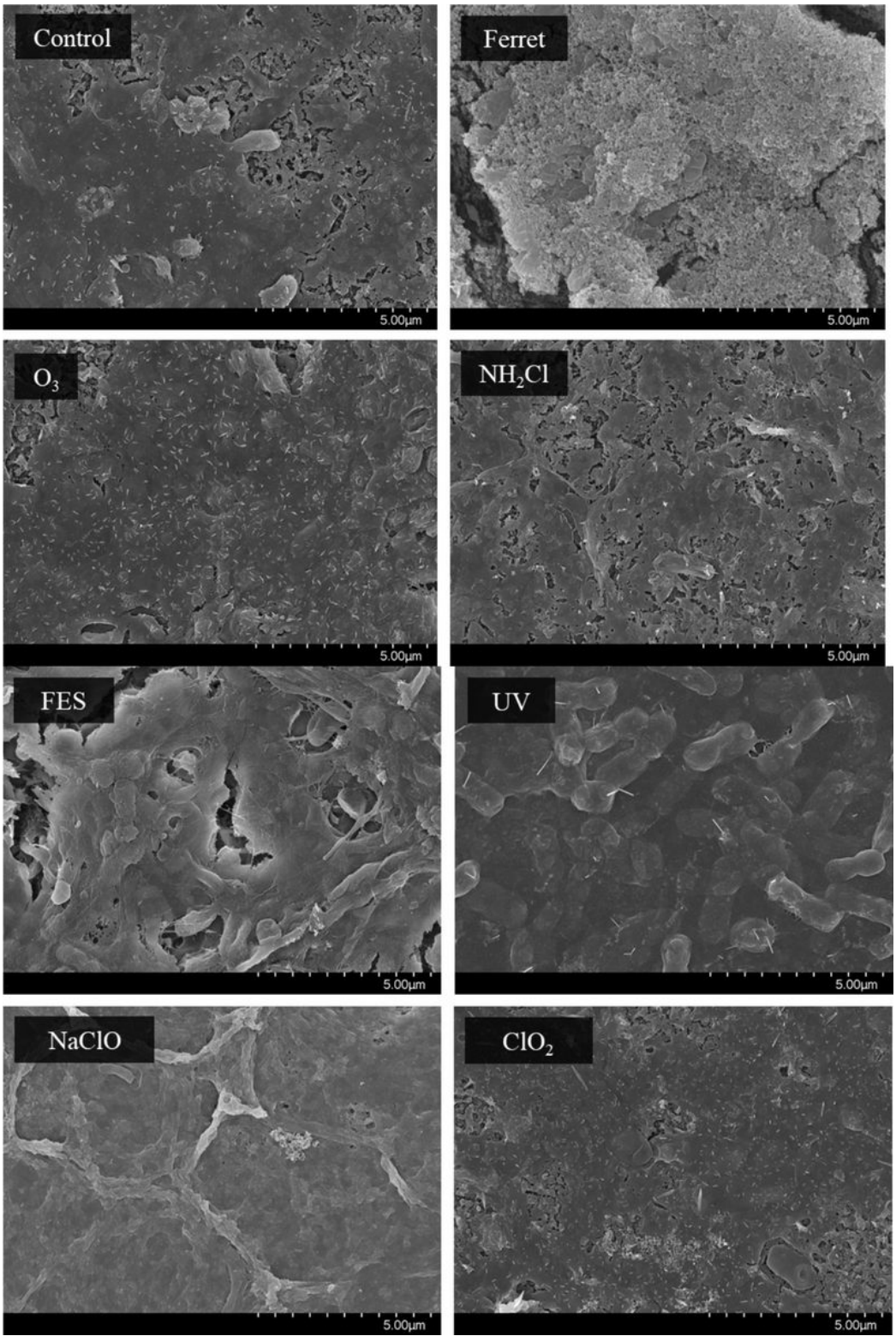

Figure 6

Scanning electron microscope (SEM) images of DRB biofilms developed on the surface of RO membranes.

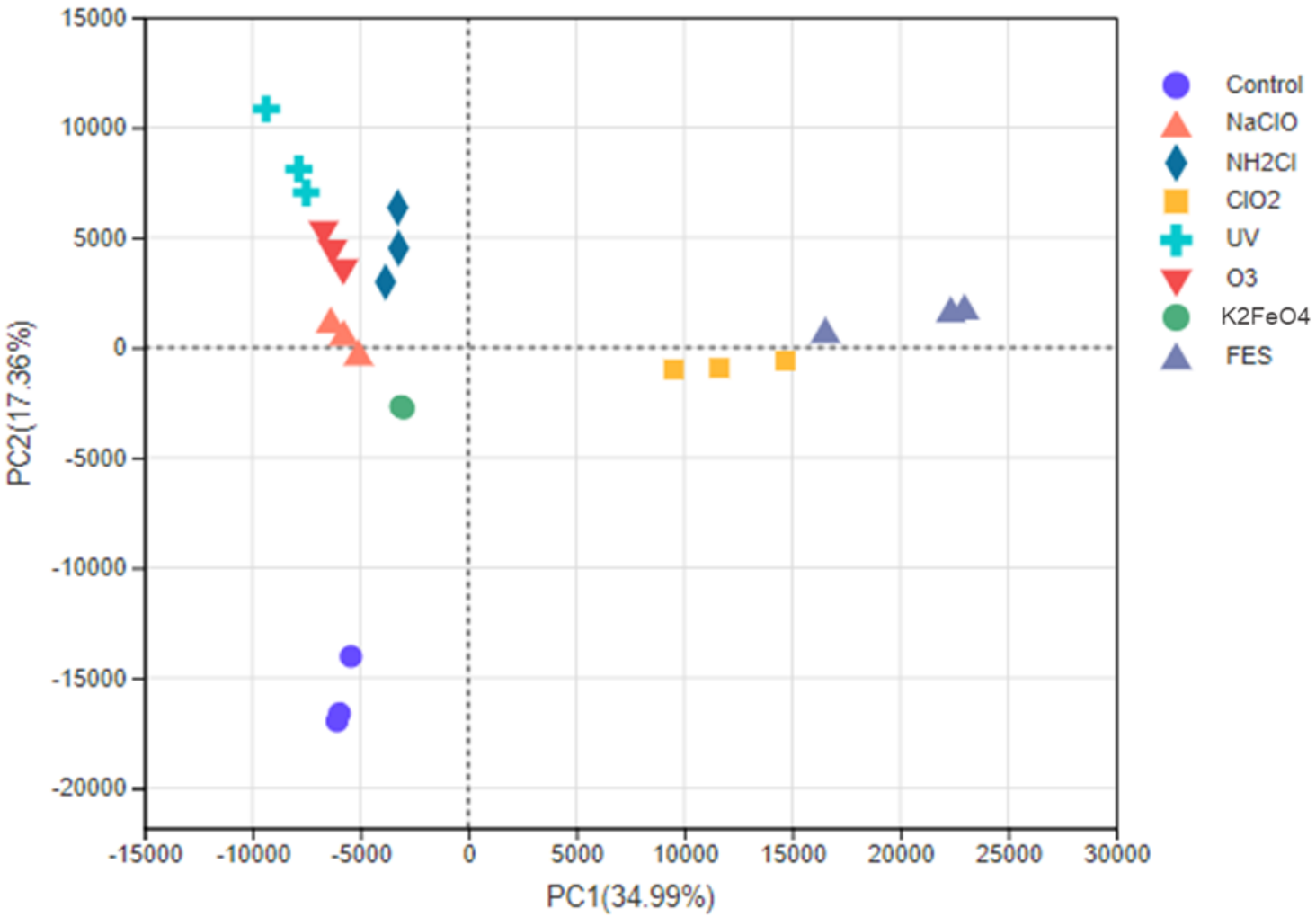

Figure 7

Principal component analysis (PCA) of microbial communities of the biofilm on the RO membranes

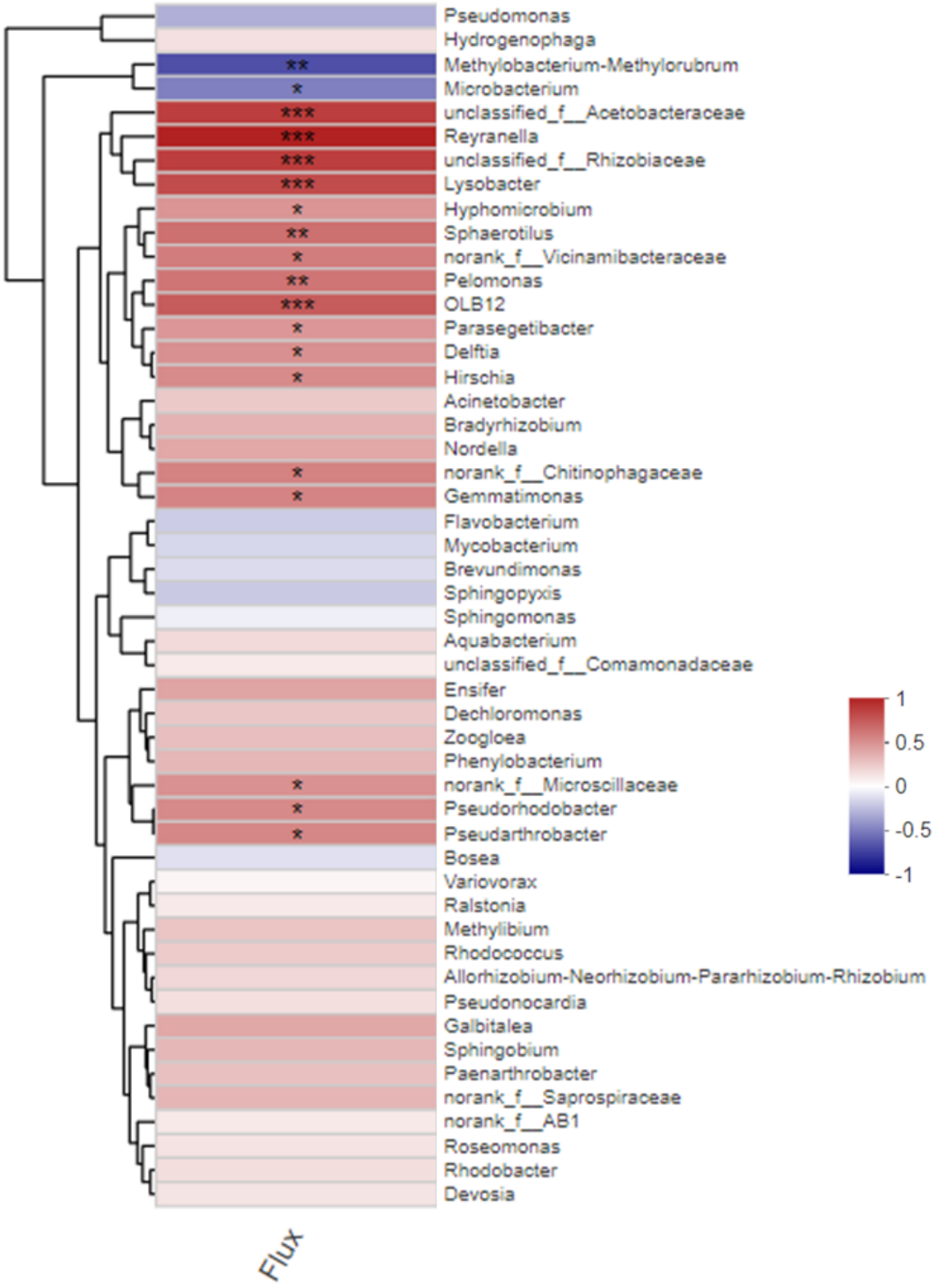

Figure 8

Heat maps of the correlation coefficient between normalised flux and relative abundance of the top 50 genera. ***, **, and * represent p<0.01, p<0.05, and p<0.1, respectively.

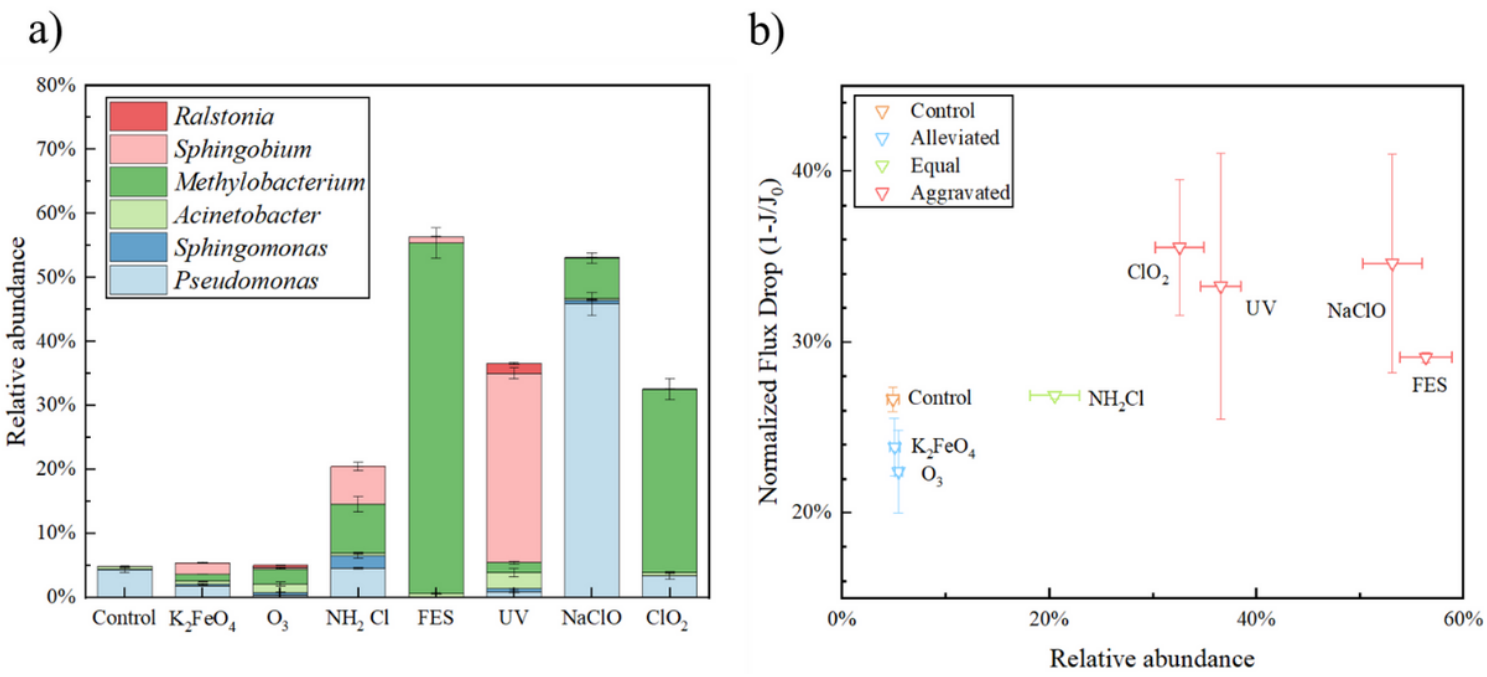

Figure 9

Accumulative relative abundance of typical highly secretory or biofouling-related genera reported by previous research (a) and its correlation with normalized flux drop of RO membranes (b).

Supplementary Files

This is a list of supplementary files associated with this preprint. Click to download.

- SI.docx